Vegetable Research

ARTICLE

Open Access

https://doi.org/10.48130/vegres-0025-0050

Vegetable Research **2026**, 6: e011

Fine mapping and candidate gene analysis of *McFPL1* regulate fruit pedicel length in bitter gourd (*Momordica* spp.)

Tao Zeng[#], Jiayi Liu[#], Zhuoxi Yang, Rui Zhang, Fan Li, Yan Lu, Chunting Yan, Jia Liu, Kailin Hu, Jiaowen Cheng[*] and Jianwen Song[*]

College of Horticulture, South China Agricultural University/Key Laboratory of Biology and Genetic Improvement of Horticultural Crops (South China), Ministry of Agriculture and Rural Affairs, Guangzhou 510642, China

[#] Authors contributed equally: Tao Zeng, Jiayi Liu

[*] Correspondence: jiaolong1015@126.com (Cheng J); songjianwen200@scau.edu.cn (Song J)

Abstract

With the advancement of agricultural mechanization, the development of crop varieties suitable for mechanized harvesting has become an important breeding objective. In bitter gourd (*Momordica charantia*), increasing fruit pedicel length (FPL) is considered a key trait for improving harvest efficiency. However, the genetic and molecular mechanisms controlling FPL remain largely unknown. In this study, two contrasting lines, 23S083 (long FPL), and 23S184 (short FPL), were selected for comparison. Microscopic analysis revealed that the longer pedicel in 23S083 was attributable to both increased cell length and number compared to 23S184. Using F_1 and F_2 populations derived from these parents, the major locus *McFPL1* was initially mapped to a 2.46 Mb region on chromosome 3 through BSA-seq. Fine mapping with 15 polymorphic markers further narrowed the candidate region to 255.059 kb. Among the 21 genes with mutations in this interval, *Moc03g21510*, which encodes an ABCG subfamily ATP-binding cassette transporter, was proposed as the most promising candidate gene. During the elongation of the fruit pedicel, the expression level of this gene was significantly higher in 23S083 than in 23S184. Sequence analysis identified 20 SNPs and eight InDels in its 3'UTR, suggesting that these variations may influence mRNA stability and thus regulate pedicel elongation. Furthermore, the co-segregating marker developed from these variations accounted for approximately 76.7% of the phenotypic variation in FPL within the natural bitter gourd population. These results provide valuable genetic insights into FPL formation and will facilitate the molecular breeding of mechanization-adapted bitter gourd varieties.

Citation: Zeng T, Liu J, Yang Z, Zhang R, Li F, et al. 2026. Fine mapping and candidate gene analysis of *McFPL1* regulate fruit pedicel length in bitter gourd (*Momordica* spp.). *Vegetable Research* 6: e011 https://doi.org/10.48130/vegres-0025-0050

Introduction

With increasing labor costs and the advancement of agricultural mechanization, expanding novel germplasm resources suitable for mechanized harvesting has become a crucial step in accelerating the process of agricultural mechanization. The key to successful mechanized harvesting lies in the accurate identification and separation of the product organs from other plant tissues. In Cucurbitaceae species, where the fruit serves as the primary product organ, an elongated pedicel can significantly improve the machine's ability to distinguish between the fruit, pedicel, and stem, thereby enhancing the efficiency and success rate of mechanized harvesting.

At present, few studies have reported the genetic basis and molecular mechanisms of fruit pedicel morphogenesis in the Cucurbitaceae family. In luffa, a mixed major gene plus polygene inheritance model was employed to analyze a six-generation population (P_1, P_2, F_1, B_1, B_2, and F_2) derived from a cross between ridge gourd and sponge gourd. The result showed FPL in luffa was D-0 (one pair of additive-dominance major gene plus additive-dominance-epistasis polygene model)[1]. In cucumber, two minor QTLs named *qfpl1.1* and *qfpl1.2*, and one major QTL named *qfpl6.1* were identified on chromosome 1 and chromosome 6, respectively[2]. In melon, *MELO3C010972*, which encodes cytokinin oxidase, was first identified to be linked to the regulation of fruit pedicel length by BSA-seq[3]. In addition, it has been reported that the cytokinin synthesis pathway is associated with the cucumber pedicel length, and that the difference in length is due to differences in zeatin content and cell number[4].

Bitter gourd (*Momordica charantia* L.; 2x = 2n = 22), belongs to the Cucurbitaceae family and the Momordica genus. It is widely cultivated in tropical and subtropical regions, including parts of East Africa, Asia, the Caribbean, and South America[5]. Bitter gourd is not only an important economic crop due to its bitter-tasting fruits but also serves as a significant medicinal plant, as modern medical research has demonstrated its anti-diabetic and antimicrobial properties[6–10].

With the advent of next-generation long-read sequencing[11,12] and its cost-effective application in bitter gourd, high-quality genome assemblies have now been generated for both cultivated varieties (OHB3-1 and Dali-11) and wild accessions (TR)[5,13–16]. These genomic resources have significantly accelerated the characterization of key agronomic traits and are advancing molecular breeding efforts in this crop. For example, *MC04g1399* was screened as the best candidate gene for fruit wart via sequence variation and expression analysis[17]. A point mutation (C277T) in the *MC06g1112* gene is associated with a decrease in the first flower node[18]. A number of interesting traits have been investigated successively. Such as stigma color[19], gynoecy[20], and seed coat color[21] in bitter gourd, and others.

However, research on fruit pedicel length (FPL) in bitter gourd remains scarce, limiting our understanding of its developmental mechanisms. In this study, a preliminary investigation using bitter gourd lines differing in fruit pedicel length were initiated, establishing a dynamic developmental model, and pinpointing the combined contribution of cell length and cell number to this morphological difference. An F_1 population and a segregating F_2

population (n = 241) were generated from a cross between the long-pedicel line 23S083, and the short-pedicel line 23S184 to explore the genetic and molecular basis of FPL in bitter gourd. To form two DNA bulks, the genomic DNA samples of individual plants with extreme phenotypes were pooled with long (30 accessions), and short (30 accessions) fruit pedicels for whole-genome resequencing. The inheritance locus was identified in a 2.46 Mb region. Then, 15 polymorphism markers were developed using resequencing data to narrow down the candidate area using the F_2 population of 1,076 individuals. *McFPL1* was genetically mapped to a 255.059 kb region harboring five annotated genes with sequence variations between the parental accessions. Combining sequence analysis and expression pattern analysis, *Moc03g21510* was proposed as the best candidate gene for *McFPL1*, which encodes an ATP-binding cassette transporter. Genotyping in a natural population suggests that *Moc03g21510* plays a significant role in regulating FPL in bitter gourd. Based on microscopic observation, *Moc03g21510* may be involved in the transport of a certain hormone[22]. Altered expression patterns lead to differential cellular responses to the hormone, thereby resulting in morphological changes in pedicel length. These findings enhance our understanding of plant hormones and their transporters.

Materials and methods

Plant materials and phenotyping

23S083 with long fruit pedicel, and 23S184 with short fruit pedicel were used to produce an F_2 segregating population for genetic mapping of fruit pedicel grown in the autumn of 2023. FPL data were systematically collected from the onset of female flowering through multiple developmental stages. Measurements were taken along the entire pedicel, from its base to the point of attachment with the stem, allowing the construction of a detailed dynamic profile of fruit pedicel development in bitter gourd. All plant materials were grown at South China Agricultural University, Guangzhou, China (23° N, 113° E).

BSA-seq analysis

The individuals exhibiting extreme phenotypes were selected from the F_2 population, and were constructed with two bulks: long-FPL and short-FPL, each comprising an equal mixture of DNA from 30 F_2 plants displaying the corresponding fruit pedicel length (FPL) phenotype. Genomic DNA was extracted from each F_2 individual, and the two parental lines (23S083 and 23S184) using the cetyltrimethylammonium bromide (CTAB) method[23]. The two bulked DNA pools and the parental lines were then subjected to whole-genome resequencing on the BGI platform. The sequencing data were calculated based on the reference genome OHB3-1 and analyzed according to a previous study[24]. The SNP-index was calculated for each variant type[25]. The SNP-index and Δ(SNP-index) for the long- and short-FPL pools were computed using a 200 kb sliding window with a 100 kb step size. Genomic regions exceeding the 95% confidence intervals in the SNP-index analyses were identified as candidate regions associated with the trait (Supplementary Table S1).

Map-based cloning analysis and fine mapping

Based on the sequence alignment results between the re-sequencing data of the two parental lines and the OHB3-1 reference genome[26], SNPs and InDels between the parental lines were developed into molecular markers to construct a linkage map for the candidate region using Primer 5 software. Ultimately, a total of 15 markers were used to construct a genetic linkage map of the candidate region for the F_2 population, using JoinMap 4[27] and MapChart[28] software. All of the primers used in this study are listed in Supplementary Table S2.

Candidate gene cloning and sequence analyses

Total RNA was extracted from young fresh leaves using the TRIzol reagent[29] (RN01, Keepbio, China). cDNA synthesis was performed using a HiScript II 1st Strand cDNA Synthesis Kit (Vazyme, Nanjing). Based on the OHB3-1 reference genome, the full-length sequence of the candidate gene was cloned. Two primer pairs were designed to amplify the full-length CDS along with the 3'UTR region of *Moc03g21510* from 23S083 and 23S184 (Supplementary Table S2). The PCR system was prepared using Phanta Max Super-Fidelity DNA Polymerase (Vazyme, Nanjing). All fragments were sequenced by Sanger sequencing at Guangzhou Tsingke Biotechnology (Guangzhou, China).

Gene expression analysis

Expression of five candidate genes was analyzed across seven tissues: root, stem, leaf, female flower, male flower, fruit, and fruit pedicel. The expression dynamics of *Moc03g21510* were further assessed in fruit pedicels at four developmental stages—two days before anthesis (2 DBA), zero days post-anthesis (0 DPA), and one day post-anthesis (1 DPA)—in both parental lines. All samples were collected with three biological replicates, snap-frozen in liquid nitrogen, and stored at −80 °C until RNA extraction. Quantitative PCR was performed using Eastep® qPCR Master Mix following the manufacturer's protocol, with three technical replicates per sample. The bitter melon actin gene *Mc01g0724* was used as the internal reference, and relative expression levels were calculated using the $2^{-\Delta\Delta CT}$ method[30].

Microscope examination of the pedicel cell

Longitudinal sections were prepared from fruit pedicels collected at four developmental stages, including the first day of the appearance of the ovary, 2 DBA, 0 DPA, and 10 DPA. Fresh tissue samples were immediately immersed in FAA fixative solution and stored for over 24 h[31]. Morphologically intact and normal materials were selected for paraffin embedding and subsequent longitudinal sectioning. The sections were stained with toluidine blue for cellular visualization. The sectioning process was performed by a commercial service provider (Servicebio®). Based on microscopic observations, the number and length of cells within a standardized area were quantified for each developmental stage.

Statistical analysis

All statistical analyses were performed using GraphPad Prism version 10.1.2 (www.graphpad.com). Two-way ANOVA with Sidak test and Student's *t*-test were used in this study. Single asterisks (* $p < 0.05$), double asterisks (** $p < 0.01$), and triple asterisks (*** $p < 0.001$) indicate statistically significant differences.

Results

Inheritance and phenotypic characterization of fruit pedicel length in bitter gourd

To characterize the fruit pedicel length (FPL) phenotype in bitter gourd, FPL in 23S083 and 23S184 were quantified using a digital

caliper, measuring from the stipule to the base of the pedicel (Fig. 1a). At fully maturity (25 DPA), the mean FPL for the long-pedicel parental 23S083 and short-pedicel parental 23S184 lines were 10.87 ± 4.03 cm and 3.77 ± 1.92 cm, respectively (Fig. 1b). The FPL of 23S083 is approximately three times that of 23S184.

To investigate the dynamic changes in FPL during the bitter gourd growth cycle, a morphological evaluation and comparative analysis between 23S083 and 23S184 were carried out throughout development, from ovary emergence to fruit maturation. Following statistical analysis, it was observed that bitter gourd FPL enters a plateau phase after pollination, with the majority of pedicel elongation occurring before anthesis, and the difference in the FPL between 23S083 and 23S184 had peaked (Fig. 1b). Approximately 92% of the total pedicel elongation was completed before

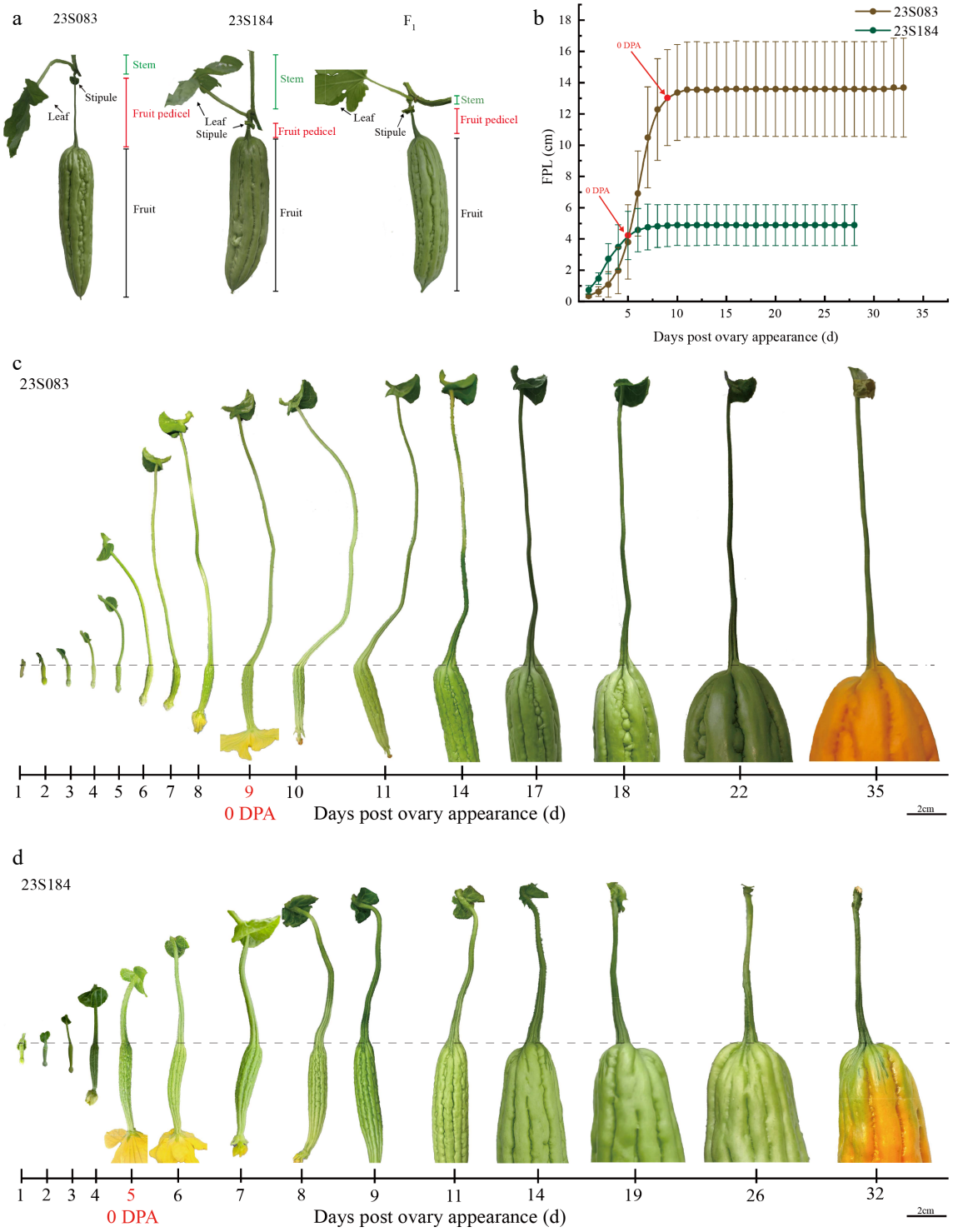

Fig. 1 Phenotypic characterization of fruit pedicel length in bitter gourd. (a) Structural characteristics of 23S083, 23S184, and their F_1 lines at commercial maturity. (b) The dynamic changes of FPL (fruit pedicel length) across developmental stages of 23S083 and 23S184 lines. Image of representative stages in the FPL changing process of (c) 23S083, and (d) 23S84.

flowering in both parents. The maximum growth rate was reached at 3 DBA and 2 DBA in 23S083 and 23S184, respectively (Fig. 1c, d).

Increased cell elongation and division are associated with a longer FPL

To explore the cytological differences between long and short pedicels, fruit pedicel samples were collected at four developmental stages, including the emergence of the ovary, the period of peak growth, 0 DPA, and 10 DPA, and longitudinal sectioning performed for histological analysis (Fig. 2a–f). The dynamic changes in pedicel elongation in lines 23S083 and 23S184 were evaluated primarily in terms of cell number and cell length.

After statistical analysis, it was found that the cell length of 23S083 increased from 24.79 to 143.36 μm, while that of 23S184 increased from 26.02 to 73.86 μm during pedicel elongation. The average cell lengths during the period of peak growth were 42.74 μm for 23S083 compared with 44.76 μm for 23S184. In 0 DPA, the capability for cell elongation was observed, with 23S083 reaching 139.70 μm and 23S184 measuring 70.72 μm. Following this period, the cell length of the long-pedicel cultivar (23S083) stabilized at approximately twice that of the short-pedicel line (23S184) (Fig. 2g; Supplementary Table S3). This sustained difference was mirrored by the greater cell elongation capacity observed in 23S083.

Since the differences in cell length alone cannot fully account for the morphological variation between 23S083 and 23S184, morphological and cell length data were combined to estimate the cell numbers at different developmental stages. At the emergence of the ovary, no significant differences were observed between 23S083 and 23S184 in terms of FPL or cell length, suggesting similar cell numbers at this stage (Figs 1b–d, 2a, d, g). During the period of peak growth, the FPL of 23S083 was approximately 2.5 times that of 23S184, while no significant difference in cell length was detected (Figs 1b–d, 2b, e, g). Therefore, it is reasonable to infer that this morphological disparity largely arises from a greater number of cells in 23S083 compared to 23S184. As the fruit pedicel elongated further, by 0 DPA, the FPL of 23S083 was about three times that of 23S184 (Fig. 1b–d). At the cellular level, 23S083 also exhibited a greater elongation capacity, with its cell length reaching twice that of 23S184 (Fig. 2c, f, g). Accordingly, the cell number in 23S083 should be significantly higher than in 23S184, aligning with the observed morphological differences. Subsequently, fruit pedicel elongation entered a plateau phase after pollination, during which changes in cell length also ceased, and cell numbers presumably stabilized at this stage (Figs 1b–d; 2g).

In summary, FPL variation was driven by the combined effects of cell number and cell length. This morphological divergence was initially driven by differential cell division, which resulted in a significantly greater cell number in line 23S083 than in 23S184 during the peak growth period. Subsequently, divergence in cell elongation capacity also contributed to the elongation of the fruit pedicel. Ultimately, the long fruit pedicel line demonstrated both greater cell numbers and increased cell length compared to the short fruit pedicel line. These findings suggest that the long-pedicel line employs a dual strategy, enhancing both cell elongation and proliferation to achieve its final length.

Initial mapping of *McFPL1* by BSA-Seq

To elucidate the genetic basis of FPL and identify the underlying genes in bitter gourd, F_1 and F_2 populations were developed from crosses between the parental lines 23S083 and 23S184. Statistical analysis revealed that the mean FPL for the F_1 (23S083 × 23S184) hybrid line, grown in the spring of 2023, was 7.22 ± 1.83 cm, falling at the midpoint between these two parental lines. The frequency distribution of fruit pedicel length (FPL) in the F_2 population exhibited considerable variation. Individuals with distinctly long and short fruit pedicels were selected from the 241 F_2 segregating population for DNA extraction to create the long and short-pedicel bulks. The two parental lines, along with the two DNA bulks, were subjected to whole-genome resequencing.

An average of 51.56 Gb of clean reads per sample was obtained, with an average sequencing depth of 41.25 (×). On average, 97.12% of reads had a Q30 quality score and were successfully mapped to the OHB3-1 reference genome[26]. After variant filtering, a total of 68,224 high-quality SNPs, and 18,334 small InDels were identified.

Based on the genomic positions of the variants and the annotated gene locations in the reference genome, SnpEff software was employed to predict the effects and functional impacts of high-quality SNPs and InDels. 68,224 high-quality SNPs, and the SNPNUM method was used to fit the Δ(SNP-index) curves. Based on the differences in the allele frequencies, the locus of the fruit pedicel length was mapped to a 2.46 Mb region, on chromosomes 3, and provisionally named it *Momordica charantia Fruit Pedicel Length 1* (*McFPL1*) (Fig. 3a; Supplementary Table S4).

McFPL1 was fine-mapped to the 255.059kb interval

To further refine the candidate region of *McFPL1* identified via BSA-seq analysis, SNPs, and InDels derived from the four DNA

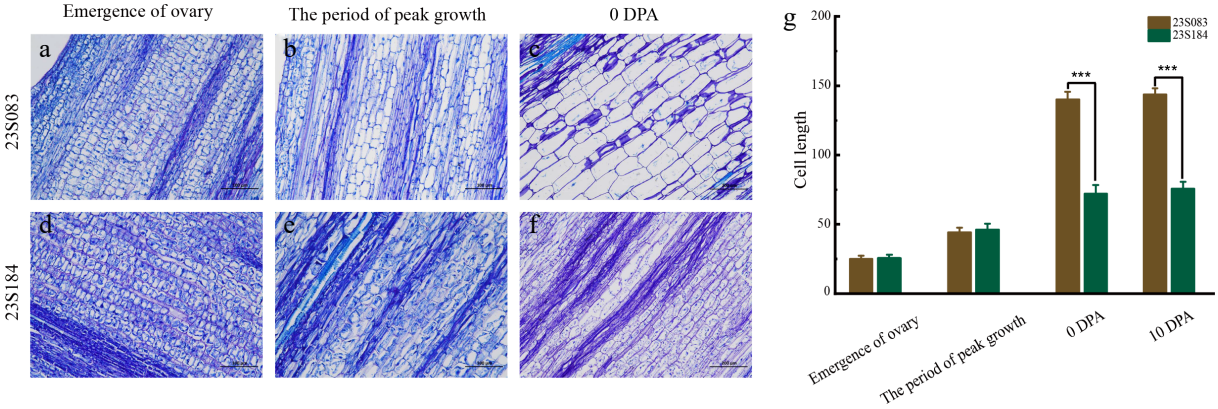

Fig. 2 Microscope evaluation of the pedicel cell. Representative cell morphology of fruit pedicel longitudinal sections at key stages in (a)–(c) 23S083, and (d)–(f) 23S184; with (g) corresponding quantifications of cell length. Data are presented as mean ± SE. *** $p < 0.001$, ** $p < 0.01$ (Student's *t*-test).

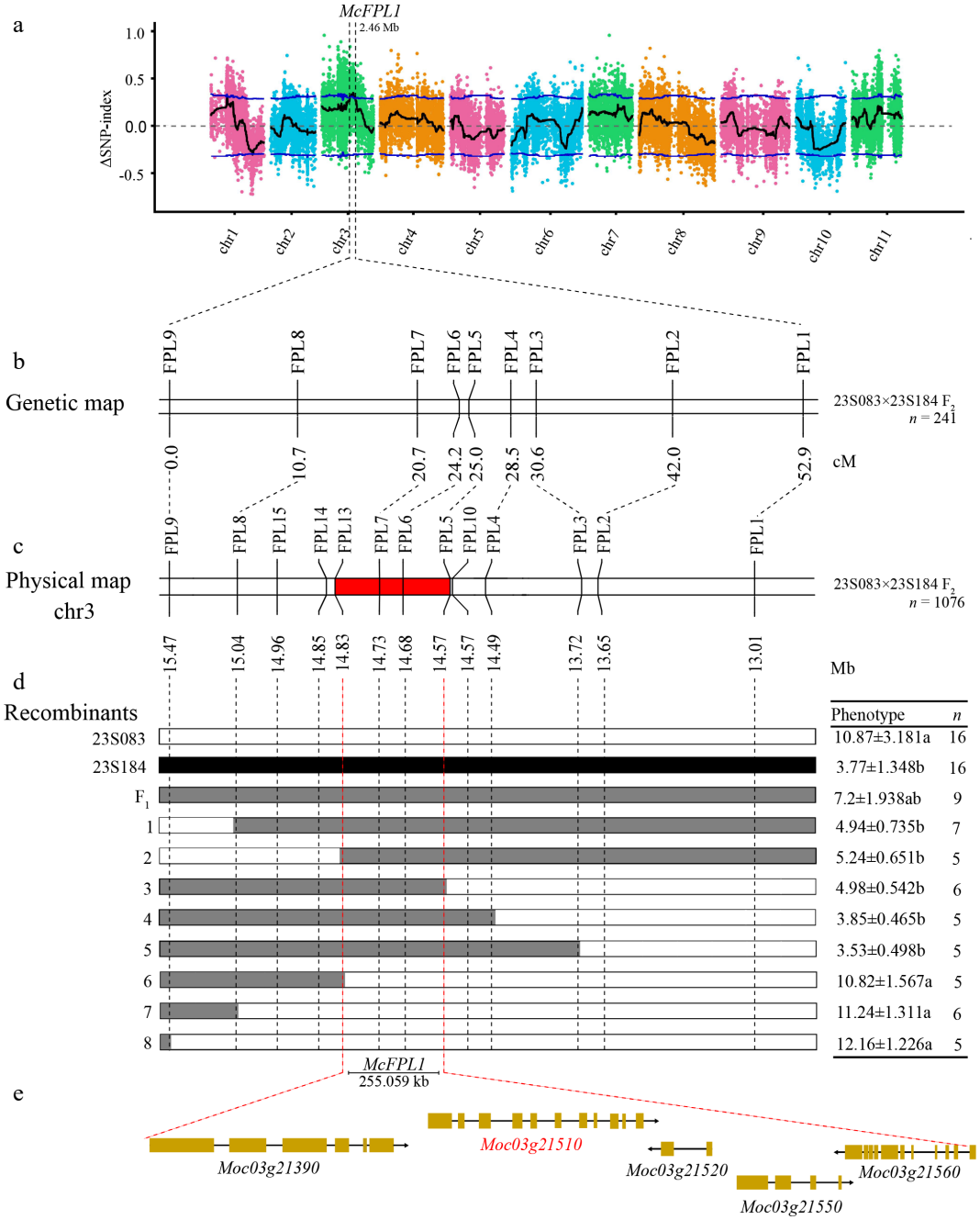

Fig. 3 Map-based cloning of *McFPL1*. (a) Manhattan plot of the ΔSNP-index. The blue line represents the threshold lines for confidence levels of 0.95. The confidence interval for *McFPL1* at 2.46 Mb on chromosome 3 is indicated by the red dotted lines. (b) Genetic linkage map of the 241 individual F_2 population (23S083 × 23S184). (c) Physical position of the markers based on the OHB3-1 reference genome, the 255.059 kb candidate region is filled in red. (d) Fine-mapping of *McFPL1* using 1076 F_2 recombinants. The black, white, and grey bars represent 23S184, 23S083, and heterozygotes, respectively. (e) The gene structure of five genes.

pools—including the parental lines 23S083 and 23S184, as well as the long and short fruit pedicel bulks—were utilized. Based on SNP and InDel information, a total of 15 polymorphic markers were developed for linkage map construction (Fig. 3b, c; Supplementary Table S2).

Combined with genotypes and phenotypes of the recombinants, the candidate region was narrowed down to a 255.059 kb interval on the reference chromosome 3. The *McFPL1* locus was delineated between markers FPL5 and FPL13, spanning from position 14,571,981 to 14,827,040 bp (Fig. 3d).

The rich variation in the 3'UTR of *Moc03g21510* may be linked to the variation in FPL

To identify candidate genes associated with FPL in bitter gourd and examine their genetic variations, resequencing data were first screened for sequence variations between the parental lines, and found that only five candidate genes contained non-synonymous mutations (Fig. 3e; Supplementary Tables S4, S5). Among them, *Moc03g21390*, *Moc03g21520*, *Moc03g21550*, and *Moc03g21560* harbored 1, 3, 1, and 1 non-synonymous mutations, respectively (Fig. 4a, c–e; Supplementary Table S4), each leading to an alteration

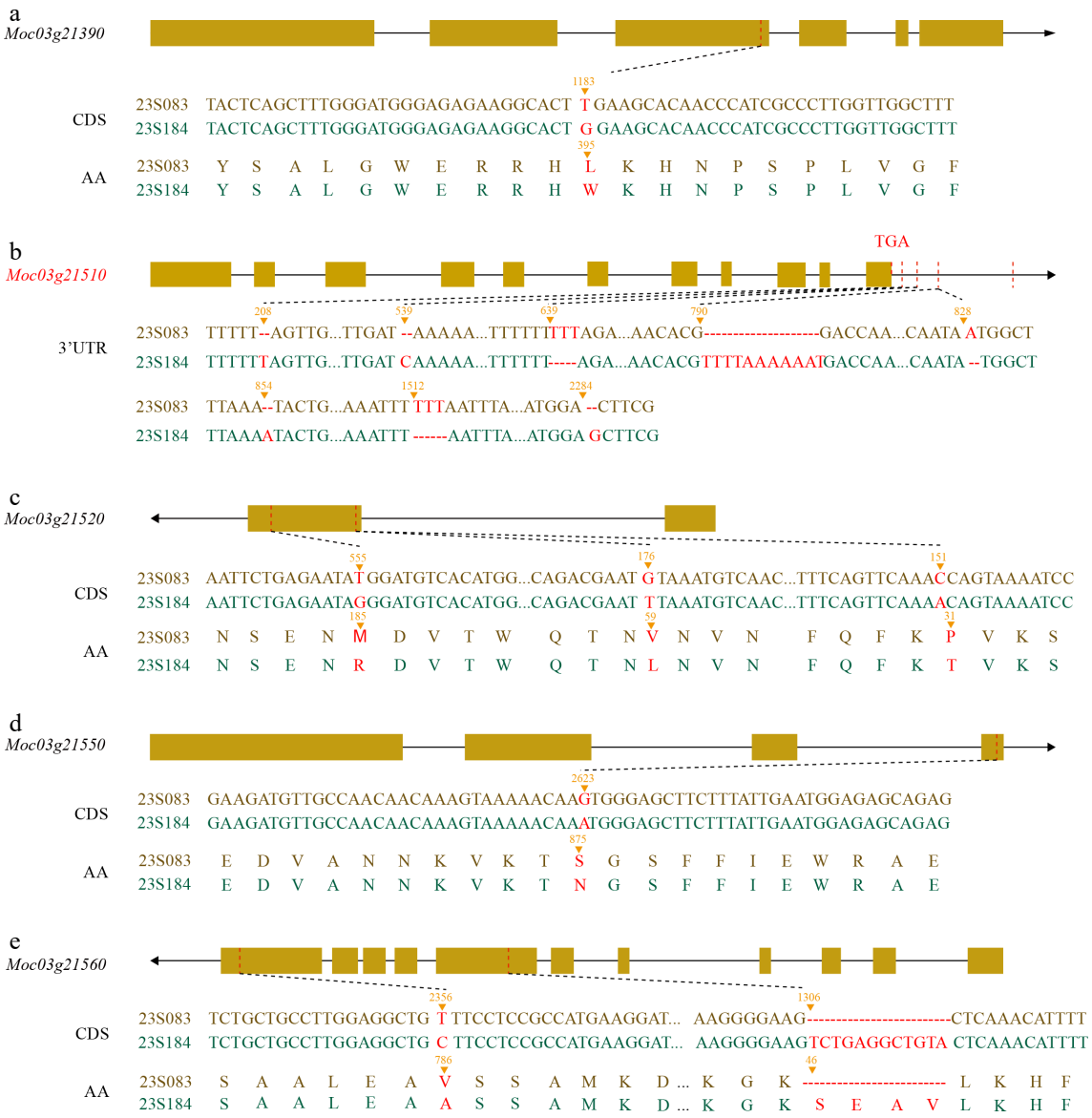

Fig. 4 (a), (c)–(e) Sequence analysis of the candidate gene. DNA sequence variations and the resulting non-synonymous amino acid changes in the four candidate genes. (b) InDel information for *Moc03g21510*. Variant positions were calculated excluding introns.

in the encoded amino acid sequence. Moreover, a 12-bp InDel was detected within the CDS of *Moc03g21560* (Fig. 4e). All identified variants were confined to the coding regions. Interestingly, genetic variation in *Moc03g21510* was localized to the 3'UTR (Fig. 4b; Supplementary Fig. S1; Supplementary Table S6). To fully characterize this gene, full-length cloning from the parental materials, obtaining complete sequences of the CDS (Supplementary Fig. S1), promoter (Supplementary Fig. S2), and 3'UTR were performed. Sequence alignment showed that additional 3'UTR variations, not previously detected, were uncovered. Relative to the OHB3-1 reference genome, the 3'UTR of *Moc03g21510* exhibited considerable divergence between accessions 23S083 and 23S184, including 20 SNPs and eight InDels (Supplementary Table S6). The pronounced sequence variation observed in the 3'UTR between parental lines is particularly noteworthy, as this region plays a critical role in post-transcriptional regulation. Such extensive structural diversity may influence mRNA stability or translation, potentially contributing to differential protein expression.

Expression patterns of *McFPL1*

To pick out the candidate gene in controlling fruit pedicel length, quantitative real-time PCR (qPCR) was performed to determine their relative expression levels across various tissues—including root, stem, leaf, petal, fruit, and fruit pedicels—at different developmental stages (2 DBP, 0 DPA, 1 DPA) (Fig. 5b–f).

The results of qPCR revealed distinct expression patterns among the candidate genes. At 2 DBA, the expression levels of *Moc03g21390*, *Moc03g21510*, and *Moc03g21520* in line 23S184 were significantly higher than those in 23S083 (Fig. 5b–d). By 0 DPA, this significant inter-parental difference persisted only for *Moc03g21510* (Fig. 5b). At 1 DPA, *Moc03g21550* and *Moc03g21560* exhibited divergent expression patterns between the parents (Fig. 5e, f). In fact, approximately 92% of the total pedicel elongation was completed before 0 days post-anthesis (DPA). The pedicel then enters a plateau phase at 1 DPA, after which there is no significant further increase in fruit pedicel length. The expression profile of *Moc03g21510*—showing significant differences at 2 DBA and 0 DPA, but not at

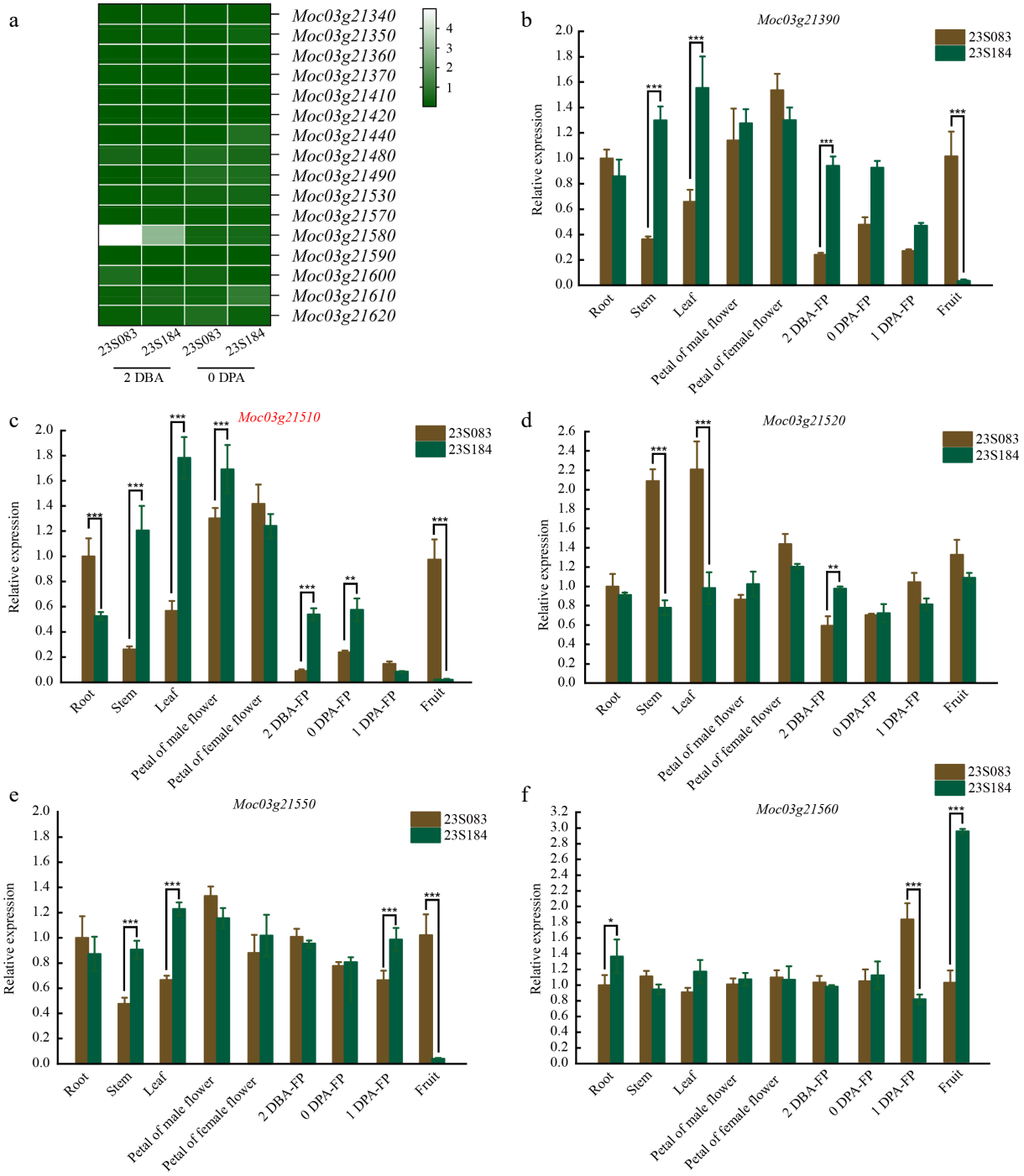

Fig. 5 Expression pattern of the candidate genes. (a) The relative expression level of 16 genes in two stages of fruit pedicel (2 DBA, 0 DPA) with a heatmap. The relative expression levels of (b) *Moc03g21390*, (c) *Moc03g21510*, (d) *Moc03g21520*, (e) *Moc03g21550*, and (f) *Moc03g21560* in root, stem, leaf, petal, fruit, and three stages of fruit pedicel (2 DBA, 0 DPA, 1 DPA). Values represent the mean ± SE of three biological replicates. Different letters (***, **, *) indicate statistically significant differences at $p < 0.001$, $p < 0.01$, and $p < 0.05$, respectively, according to the Sidak test.

1 DPA—uniquely correlated with the phenotypic dynamics, thus identifying it as the prime candidate (Fig. 5c). It also exhibited significant differences in most tissues, except in the petal of the female flower, providing strong evidence that structural variations in its 3'UTR influence its expression regulation. Additionally, the expression level of other genes with non-coding variations in the 255.059 kb interval between two key stages of fruit pedicel elongation (2 DBA and 0 DPA) were evaluated, and it was found that the expression profiles of these genes were not correlated with the phenotypic dynamics (Fig. 5a). Taken together, *Moc03g21510* was proposed as a gene associated with FPL in bitter gourd.

McFPL1 locus can explain approximately 76.7% FPL phenotypes in bitter gourd natural population

To elucidate the genetic mechanism of fruit pedicle length in bitter gourd, a co-segregating marker was developed based on an

11 bp InDel in the 3'UTR of *Moc03g21510* (Fig. 6a–c; Supplementary Tables S2, S6). This marker was used to genotype 42 bitter gourd accessions, and their FPL was measured based on the evaluation of phenotypic data from 23S083 and 23S184. Genotyping results indicated that this co-segregating marker could explain 76.7% of the phenotypic variation in a natural population of bitter gourd (Supplementary Table S7). This high consistency not only confirms the strong association between *McFPL1* and FPL, but also suggests that additional genes are involved in the regulation of FPL in bitter gourd.

Discussion

Fruit pedicel length (FPL) is an important trait influencing the success rate of mechanized harvesting in cucurbit crops. Although a little progress has been made in understanding FPL within the cucurbit family, the molecular mechanisms controlling FPL in bitter gourd remain largely unknown, and current knowledge regarding its genetic regulation is still limited.

In this study, the parental lines 23S083 and 23S184, along with their derived F_2 population, were utilized to map a quantitative trait locus (QTL) controlling FPL, named *McFPL1*, via bulked segregant analysis. *McFPL1* was initially mapped to a region of 2.46 Mb on chromosome 3. Using 15 polymorphic markers, a genetic linkage map was constructed, enabling the refinement of *McFPL1* to a 255.059 kb interval containing five genes in which sequence variations were detected between the parental lines. Based on gene annotation, enriched metabolic pathways, and resequencing data, in conjunction with a comprehensive analysis of gene expression levels throughout fruit pedicel development, the findings strongly suggest, *Moc03g21510*, which encodes an ABC transporter family protein, as the gene responsible for controlling FPL in bitter gourd. This conclusion was further substantiated by genotyping results derived from a natural population of 42 bitter gourd accessions.

Research on the molecular genetic mechanisms underlying fruit pedicel length in cucurbit crops has made little progress. In the exploration of molecular mechanisms regulating FPL, genes involved in the cytokinin biosynthesis pathway have been reported to modulate FPL in cucumber[4]. Two minor-effect QTLs for FPL were detected on chromosome 1, and one major-effect QTL, designated *qfpl6.1*, was identified on chromosome 6 in cucumber, which plays a central role in the auxin signaling transduction pathway[2]. In melon, the cytokinin oxidase gene *MELO3C010972* was first proposed as a candidate gene for FPL regulation via BSA-seq[3]. These findings suggest that metabolic and signaling pathways related to cytokinin and auxin may be associated with natural variation in FPL across cucurbit species.

During the formation of the fruit pedicel, bitter gourd exhibits distinct characteristics within the cucurbit family. Unlike the morphogenetic pattern of pedicel development in melon, where the majority of fruit pedicel elongation occurs after pollination and reaches a plateau around 30 days post-pollination (DPP)[3], bitter gourd undergoes its primary FPL increase before pollination and enters a plateau phase on 1 DPA. Additionally, our study found that bitter gourd has a shorter maturation time compared to most other cucurbits (Fig. 1b–d). These traits make it particularly well-suited for use as a model plant within the cucurbit family.

At the cellular level, studies in cucumber and melon suggest that differences in FPL are mainly attributable to variation in cell number between long- and short-pedicel parents. Longitudinal sections of parental pedicels indicate that long-pedicel accessions contain significantly more cells than short-pedicel ones[2–4]. A similar disparity in cell number has also been observed in bitter gourd. In addition to cell division, cell elongation plays a significant role in determining the variation in FPL. At 1 DPA, compared to line 23S184, line 23S083 exhibits longer cells as well as a higher cell count (Fig. 2g). Collectively, both cell division and cell elongation ultimately contribute to the differences in FPL in bitter gourd. These findings suggest that the molecular mechanism controlling FPL in bitter gourd may differ from previously established models.

Sequence and expression analyses of *Moc03g21510* provide supporting evidence for its hypothesized role in regulating fruit pedicel length in bitter gourd. It has been established that the structure of the 3'-untranslated region (3'UTR) influences mRNA stability and transcript abundance. The 3'UTR may destabilize the mRNA, resulting in a reduction in its transcript level[32]. A total of 20 SNP variants and eight InDels were identified within the 3'UTR of *Moc03g21510* (Fig. 4b; Supplementary Table S6). Combined with its expression profile, we speculate that these variations may alter the secondary structure of the 3'UTR[33], thereby affecting gene expression levels and ultimately contributing to differences in pedicel length.

The ATP-binding cassette (ABC) transporter family represents one of the largest protein families in plants and is involved in the

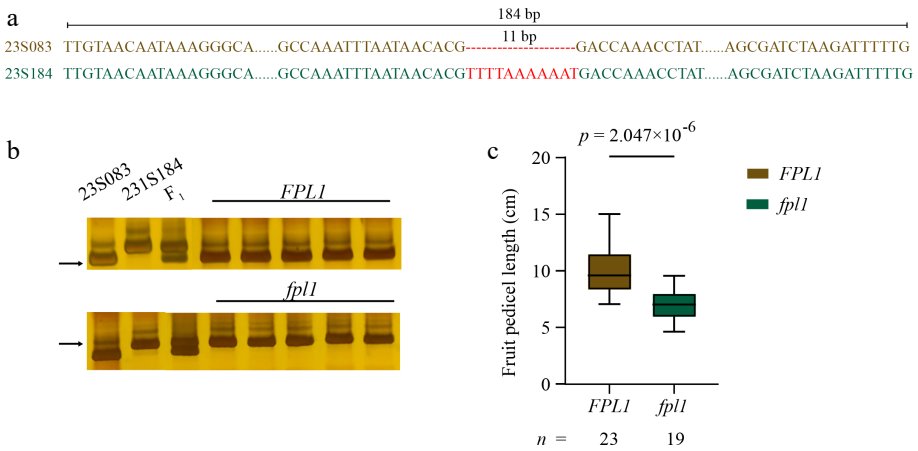

Fig. 6 Genotyping of bitter gourd natural populations. (a) The sequence deletion in *McFPL1* between 23S083 and 23S184 was employed for genotyping. (b) Representative polyacrylamide gel electrophoresis (PAGE) of *McFPL1* PCR products. (c) Comparison of fruit pedicel length between the two genotypes in a natural population. Statistical significance was assessed using a *t*-test.

transport of a wide range of substances, including hormones, defense-related secondary metabolites, and lipidic molecules, playing essential roles in numerous physiological processes[34–38]. ABC proteins typically contain nucleotide-binding domains (NBDs) and transmembrane domains (TMDs). The NBDs feature several highly conserved motifs, while TMDs are more variable. ABC transporters can be classified as full-size (containing two TMDs and two NBDs) or half-size (with one TMD and one NBD). Half-size transporters often dimerize with other half-size proteins to form functional complexes, contributing to the diversity of transport substrates, whereas full-size ABC proteins can function independently. The variability in their TMDs is precisely what enables the translocation of a diverse range of substrates[35,39,40].

Notably, *Moc03g21510* encodes a full-size ABC transporter. Genetic variations within its 3'UTR, coupled with altered expression patterns, suggest that sequence polymorphisms may influence its transcriptional regulation, potentially leading to changes in protein abundance rather than modifying substrate specificity via changes to the CDS. Such alterations could affect the transport of specific substrates and thereby contribute to natural variation in fruit pedicel length. Further studies are needed to definitively identify its transport substrates and to elucidate the mechanism through which this process regulates FPL in bitter gourd.

Conclusions

In this study, the parental lines of bitter gourd with contrasting fruit pedicel lengths (23S083 and 23S184) were investigated to elucidate the patterns of pedicel formation at both morphological and cellular levels. It was found that differences in cell elongation and division capabilities contribute to the variation in fruit pedicel length (FPL) in bitter gourd. Through bulked segregant analysis, a gene controlling fruit pedicel length was mapped to a region of 255.059 kb on chromosome 3. Subsequent sequence and expression analyses identified *Moc03g21510,* which encodes an ABC transporter, as the most promising candidate gene. The genetic variation in the 3'UTR of *Moc03g21510* between 23S083 and 23S184 may alter the transport of specific substrates, thereby affecting fruit pedicel elongation in bitter gourd. These findings provide new insights into the morphogenesis of pedicel in cucurbit crops and offer novel perspectives on the molecular mechanisms controlling pedicel elongation, deepening our understanding of this developmental process.

Author contributions

The authors confirm their contributions to the paper as follows: study conception and design: Song J, Cheng J, Hu K, Zeng T, Liu JY; data collection: Zeng T, Liu JY, Yang Z, Zhang R, Li F, Lu Y, Yan C, Liu J; analysis and interpretation of results: Song J, Zeng T, Liu JY; draft manuscript preparation: Song J, Zeng T, Liu JY. All authors reviewed the results and approved the final version of the manuscript.

Data availability

The data that support the findings of this study are available in the CuGenDBv2 (http://cucurbitgenomics.org/v2/), and NBCI (www.ncbi.nlm.nih.gov). These data were derived from the following resources available in the public domain: *Moc03g21390* (XP_022152851.1), *Moc03g21510* (XP_022152836.1), *Moc03g21520*, *Moc03g21550*, *Moc03g21560*.

Acknowledgments

This work was supported by grants from the National Natural Science Foundation of China (32302535), the Guangdong Basic and Applied Basic Research Foundation (2024A1515010470, 2026A1515010830), the Seed Industry Revitalization Project of Special Funds for Provincial Rural Revitalization Strategy (2024-NPY-00-023, 2025-NPY-03-002), and the Science and Technology Planning Project of Guangdong Province (2022B0202160015).

Conflict of interest

The authors declare that they have no conflict of interest.

Supplementary information accompanies this paper online at: https://doi.org/10.48130/vegres-0025-0050.

Dates

Received 2 November 2025; Revised 13 December 2025; Accepted 19 December 2025; Published online 26 March 2026

References

[1] Cui J, Cheng J, Tan S, Li W, Wang G, et al. 2014. Genetic analysis of fruit length and fruit stalk length in luffa. *Guangdong Agricultural Sciences* 8:52−56 (in Chinese)

[2] Song ZC, Miao H, Zhang S, Wang Y, Zhang SP, et al. 2016. Genetic analysis and QTL mapping of fruit peduncle length in cucumber (*Cucumis sativus* L.). *PLoS One* 11:e0167845

[3] Cui H, Ding Z, Zhu Z, Liu S, Wang X, et al. 2022. Identification of major-effect QTL CmFpl3.1 controlling fruit pedicel length in melon (*Cucumis melo* L.). *Scientia Horticulturae* 293:110717

[4] Shi Y, Ding Z, Sun C, Ba D, Cui H. 2024. Cytokinin-related genes regulate cucumber fruit pedicel length. *Scientific Reports* 14:23361

[5] Schaefer H, Renner SS. 2010. A three-genome phylogeny of Momordica (*Cucurbitaceae*) suggests seven returns from dioecy to monoecy and recent long-distance dispersal to Asia. *Molecular Phylogenetics and Evolution* 54:553−560

[6] Grover JK, Yadav SP. 2004. Pharmacological actions and potential uses of *Momordica charantia*: a review. *Journal of Ethnopharmacology* 93:123−132

[7] Krawinkel MB, Ludwig C, Swai ME, Yang RY, Chun KP, et al. 2018. Bitter gourd reduces elevated fasting plasma glucose levels in an intervention study among prediabetics in Tanzania. *Journal of Ethnopharmacology* 216:1−7

[8] Chai Y, Sun Y. 2025. Advances in the biosynthesis, gene mining, and molecular mechanisms of cucurbitacin in Cucurbitaceae crops. *Vegetable Research* 5:e001

[9] Zakaria NH, Abdul Majid FA, Fadhlina A, Abdul Hamid SN, Anuar MNN, et al. 2024. Proliv Essence-3 (PE3): a nutricosmetic botanical blend as a dietary beverage for skin wellness and general health. *Beverage Plant Research* 4:e016

[10] Mohkami Z, Kheiry A, Sanikhani M, Razavi F, Tavakolizadeh M, et al. 2024. Enhancing the medicinal properties and phytochemical content of bitter melon (*Momordica charantia* L.) through elicitation with brassinosteroid, ethrel, and carrageenan. *BMC Plant Biology* 24:967

[11] Levy SE, Boone BE. 2019. Next-generation sequencing strategies. *Harbor Perspectives in Medicine* 9:a025791

[12] McCombie WR, McPherson JD, Mardis ER. 2019. Next-generation sequencing technologies. *Cold Spring Harbor Perspectives in Medicine* 9:a036798

[13] Chetri BK, Sonu SS, Shelke RG, Mitra S, Rangan L. 2025. Plastome genomics of the crop wild relative *Thladiantha cordifolia* illuminates the evolution and phylogeny of the gourd family (*Cucurbitaceae*). *Genetic Resources and Crop Evolution* 72:10441−10456

[14] Cui J, Yang Y, Luo S, Wang L, Huang R, et al. 2020. Whole-genome sequencing provides insights into the genetic diversity and domestication of bitter gourd (*Momordica* spp.). *Horticulture Research* 7:85

[15] Fu A, Zheng Y, Guo J, Grierson D, Zhao X, et al. 2023. Telomere-to-telomere genome assembly of bitter melon (*Momordica charantia* L. var. *abbreviata* Ser.) reveals fruit development, composition and ripening genetic characteristics. *Horticulture Research* 10:uhac228

[16] Matsumura H, Hsiao MC, Lin YP, Toyoda A, Taniai N, et al. 2020. Long-read bitter gourd (*Momordica charantia*) genome and the genomic architecture of nonclassic domestication. *Proceedings of the National Academy of Sciences of the United States of America* 117:14543–14551

[17] Liu J, Cui J, Dong J, Zhong J, Zhong C, et al. 2024. A 1-bp deletion in the MC04g1399 is highly associated with failure to produce fruit wart in bitter gourd. *Horticultural Plant Journal* 10:171–180

[18] Zhong J, Cui J, Miao M, Hu F, Dong J, et al. 2023. A point mutation in MC06g1112 encoding FLOWERING LOCUS T decreases the first flower node in bitter gourd (*Momordica charantia* L.). *Frontiers in Plant Science* 14:1153208

[19] Zhan J, Zhong J, Cheng J, Wang Y, Hu K. 2023. Map-based cloning of the APRR2 gene controlling green stigma in bitter gourd (*Momordica charantia*). *Frontiers in Plant Science* 14:1128926

[20] Zhong J, Cui J, Liu J, Zhong C, Hu F, et al. 2023. Fine-mapping and candidate gene analysis of the Mcgy1 locus responsible for gynoecy in bitter gourd (*Momordica* spp.). *Theoretical and Applied Genetics* 136:81

[21] Zhong J, Cheng J, Cui J, Hu F, Dong J, et al. 2022. MC03g0810, an important candidate gene controlling black seed coat color in bitter gourd (*Momordica* spp.). *Frontiers in Plant Science* 13:875631

[22] Hwang JU, Song WY, Hong D, Ko D, Yamaoka Y, et al. 2016. Plant ABC transporters enable many unique aspects of a terrestrial plant's lifestyle. *Molecular Plant* 9:338–355

[23] Murray MG, Thompson WF. 1980. Rapid isolation of high molecular weight plant DNA. *Nucleic Acids Research* 8:4321–4325

[24] Pang H, Ai J, Wang W, Hu T, Hu H, et al. 2024. Fine mapping of QTL-*fl3.1* reveal *SmeFL* as the candidate gene regulating fruit length in eggplant (*Solanum melongena* L.). *Vegetable Research* 4:e028

[25] Takagi H, Abe A, Yoshida K, Kosugi S, Natsume S, et al. 2013. QTL-seq: rapid mapping of quantitative trait loci in rice by whole genome resequencing of DNA from two bulked populations. *The Plant Journal* 74:174–183

[26] Urasaki N, Takagi H, Natsume S, Uemura A, Taniai N, et al. 2017. Draft genome sequence of bitter gourd (*Momordica charantia*), a vegetable and medicinal plant in tropical and subtropical regions. *DNA Research* 24:51–58

[27] Stam P. 1993. Construction of integrated genetic linkage maps by means of a new computer package: Join Map. *The Plant Journal* 3:739–744

[28] Voorrips RE. 2002. MapChart: software for the graphical presentation of linkage maps and QTLs. *The Journal of Heredity* 93:77–78

[29] Chomczynski P, Sacchi N. 1987. Single-step method of RNA isolation by acid guanidinium thiocyanate-phenol-chloroform extraction. *Analytical Biochemistry* 162:156–159

[30] Livak KJ, Schmittgen TD. 2001. Analysis of relative gene expression data using real-time quantitative PCR and the $2^{-\Delta\Delta CT}$ method. *Methods* 25:402–408

[31] Brandizzi F. 2000. Ruzin SE. 1999. *Plant microtechnique and microscopy*. 322 pp. Oxford, New York: Oxford University Press. £32.50 (softback). *Annals of Botany* 86:708

[32] Zhang D, Ai G, Ji K, Huang R, Chen C, et al. 2024. *EARLY FLOWERING* is a dominant gain-of-function allele of *FANTASTIC FOUR 1/2c* that promotes early flowering in tomato. *Plant Biotechnology Journal* 22:698–711

[33] Zhang T, Li C, Zhu J, Li Y, Wang Z, et al. 2024. Structured 3' UTRs destabilize mRNAs in plants. *Genome Biology* 25:54

[34] Borghi L, Kang J, Ko D, Lee Y, Martinoia E. 2015. The role of ABCG-type ABC transporters in phytohormone transport. *Biochemical Society Transactions* 43:924–930

[35] Do THT, Martinoia E, Lee Y, Hwang JU. 2021. 2021 update on ATP-binding cassette (ABC) transporters: how they meet the needs of plants. *Plant Physiology* 187:1876–1892

[36] Liu L, Zhao L, Chen P, Cai H, Hou Z, et al. 2020. ATP binding cassette transporters ABCG1 and ABCG16 affect reproductive development via auxin signalling in *Arabidopsis*. *The Plant Journal* 102:1172–1186

[37] Park J, Lee Y, Martinoia E, Geisler M. 2017. Plant hormone transporters: what we know and what we would like to know. *BMC Biology* 15:93

[38] Li Z, Yu X, Zhang K, Zhang Y. 2025. ABCG transporters in phytohormone dynamics: mechanisms, challenges, and future perspectives. *Plant Hormones* 1:e021

[39] Geisler MM. 2024. Embracing substrate multispecificity in plant ABC transporters. *Molecular Plant* 17:990–992

[40] Lefevre F, Boutry M. 2018. Towards identification of the substrates of ATP-binding cassette transporters. *Plant Physiology* 178:18–39